Journal of Molecular Catalysis A: Chemical 294 (2008) 27–36

Contents lists available at ScienceDirect

Journal of Molecular Catalysis A: Chemical

journal homepage: www.elsevier.com/locate/molcata

Preparation, characterization, and methane total oxidation of $AAl_{12}O_{19}$ and $AMAl_{11}O_{19}$ hexaaluminate catalysts prepared with urea combustion method

Fengxiang Yin, Shengfu Ji*, Pingyi Wu, Fuzhen Zhao, Chengyue Li*

State Key Laboratory of Chemical Resource Engineering, Beijing University of Chemical Technology, 15 Beisanhuan Dong Road, P.O. Box 35, Beijing 100029, China

ARTICLE INFO

Article history:
Received 29 December 2007
Received in revised form 27 April 2008
Accepted 19 May 2008
Available online 11 June 2008

Keywords:
Hexaaluminates
Urea combustion
Methane catalytic combustion
XRD
TPR

ABSTRACT

A series of $AAl_{12}O_{19}$ (A = La, Sr, Ba, Ca, Ce), $AMAl_{11}O_{19}$ (A = La, Sr; M = Cu, Mn, Fe, Ni, Mg) and $Sr_{1-x}La_xMnAl_{11}O_{19}$ (x = 0.2–0.8) hexaaluminates were prepared successfully using urea combustion method. The influences of the molar ratio (R) of urea to the total metal ions in hexaaluminates and the urea combustion temperature on the formation of the hexaaluminates were investigated. The structure of the hexaaluminates was characterized using X-ray powder diffraction (XRD) and temperature-programmed reduction (TPR). The catalytic activity for methane combustion was evaluated. The results indicated that the preparation conditions were: for $LaAl_{12}O_{19}$, the value of R was 3, the combustion time was in the range from 40 to 60 min, and the combustion temperature was not less than 500 °C; For $LaFeAl_{11}O_{19}$ and $LaMnAl_{11}O_{19}$, the value of R was 3–7, the combustion time was 40 min, and the combustion temperature was less than 500 and 400 °C, respectively; for $AAl_{12}O_{19}$ (A = Sr, Ba, Ca, Ce), $LaMAl_{11}O_{19}$ (M = Cu, Ni, Mg), $SrMAl_{11}O_{19}$ (M = Cu, Mn, Fe, Ni, Mg) and $Sr_{1-x}La_xMnAl_{11}O_{19}$ (x = 0.2–0.8), the value of R was 3, the combustion time was 40 min, and the combustion temperature was 500 °C. The prepared hexaaluminates had pure hexaaluminate phase structure and excellent catalytic activity in the methane combustion.

1. Introduction

Recently the high temperature catalytic combustion of methane has received considerable attention because of the more efficient burning in wider air-to-fuel ratio and with lower NO_x emissions than the conventional thermal combustion. Methane combustion has been proposed for many industrial applications, such as gas turbine, jet engines, etc. In these applications, the operation temperature is in the range of 1000–1400 °C. Therefore, the major difficulty is the development of a practical catalyst with high temperature stability and low temperature activity [1–3]. Supported noble catalysts are well known to be active for methane combustion. But their commercial exploitation is hampered due to decomposition, poisoning and cost [4,5]. Perovskite-type oxide catalysts exhibit high activity and thermal stability for catalytic combustion of methane. However, their specific surface areas are very low, limiting to some extent application in systems with high gas hourly space velocity (GHSV), such as methane combustion reaction [6].

Hexaaluminate materials containing alkali, alkaline earth or rare earth metal have β-Al_2O_3 or magnetoplumbite-type crystal structure. This structure consists of alternate stacking of a spinel block with close packed oxide ions and a mirror plane with the large cation. The oxygen diffusion along the perpendicular c-direction is faster in a hexaaluminate crystal than that along the perpendicular c-direction. Therefore, mirror planes are expected as a preferential diffusion route of oxide ion. The crystal growth along the perpendicular c-direction should be, therefore, suppressed to crystallize in thin plate-like morphology. Due to this anisotropic crystal shape and mass diffusion, a large surface area can be maintained at high temperature. Therefore, hexaaluminate materials have been reported to be promising catalysts for high temperature catalytic combustion due to their high catalytic activity, excellent thermal stability and high heat-resistant [7]. However, generally, hexaaluminates are difficult to prepare. Furthermore, the preparation methods have a significant influence on the properties of hexaaluminates. Hence, in order to obtain hexaaluminates with excellent property, many researchers have recently made great efforts to find some proper methods to prepare hexaaluminates. The solid-state reaction method [8,9] is simple. But this method requires high calcination temperature and long calcination time. Furthermore, this method easily leads to formation of other crystal structure, which decreases the performance of the materials. The alkoxide hydrolysis method [10–12] can prepare hexaaluminates with high specific surface area. However, this method requires complicated synthetic steps, expensive reagents. Moreover, this method has

* Corresponding authors. Tel.: +86 10 64412054; fax: +86 10 64419619.
E-mail addresses: jisf@mail.buct.edu.cn (S. Ji), licy@mail.buct.edu.cn (C. Li).

1381-1169/$ – see front matter © 2008 Elsevier B.V. All rights reserved.
doi:10.1016/j.molcata.2008.05.015

stringent requirements like control of pH, temperature, etc. The co-precipitation method [7,13–15] can also prepare hexaaluminates whose performance is almost the same as that of hexaaluminates by the alkoxide hydrolysis method. But the co-precipitation method is very difficult to prepare transition metal cations substituted hexaaluminates. The reverse microemulsion method [16,17] can prepare hexaaluminates with ultrahigh specific surface areas. However, this method has many disadvantages: very complicated synthetic steps, long synthetic time, low yield of products, high cost and difficulty in preparing transition metal cations substituted hexaaluminates. Accordingly, the commercial exploitation of this method is hampered. The template method [18] comes from the synthesis of mesoporous materials. But this method is very complicated, and templates have a significant influence on the performance of the hexaaluminates. Though these methods have been employed to prepare hexaaluminates with excellent catalytic activity, they cannot be applied to a large-scale and economic production because they require high calcination temperature (about 1200 °C), long calcination time (about 5 h), complicated synthetic steps, high energy cost and some expensive and toxic reagents which cause environmental pollution.

In recent years, combustion method [19–24] has been widely employed to produce cermet [25–27], solid solutions [24,28–30], perovskite-type oxides [20,31] and spinel [32–34] because it is a quite simple, fast, inexpensive and less energy cost preparation route without the intermediate decomposition and/or calcining steps. The method exploits an exothermic, usually very rapid and self-sustaining chemical reaction between oxidizers and fuels, which is ignited at a temperature much lower than the actual phase transformation temperature. Its key feature is that the heat required to drive the chemical reaction and accomplish the compound synthesis is provided by the reaction itself and not by an external source [31,35]. Usually, the desired metal nitrate salts are used as the oxidizers and various organic compounds, such as urea, citric acid, carbohydrazide, glycine and alanine, as the fuels. For most purposes, urea is the most convenient fuel to use: it is readily available commercially, is cheap, and generates the highest temperature [20,31]. In previous work, we prepared Co–Mg solid solutions [36], Ce–La solid solutions [37] and scheelites [38] by urea combustion method, and these materials exhibit excellent catalytic activity for the combustion of methane. However, as far as we know, there is no report on hexaaluminates prepared by urea combustion method. In this study, a series of $AAl_{12}O_{19}$ (A = La, Sr, Ba, Ca, Ce), $AMAl_{11}O_{19}$ (A = La, Sr; M = Cu, Mn, Fe, Ni, Mg) and $Sr_{1-x}La_xMnAl_{11}O_{19}$ (x = 0.2–0.8) hexaaluminates were quickly prepared at low temperature by urea combustion method. The aim is to apply the urea combustion method to the preparation of hexaaluminates, and develop a new and environmentally friendly preparation method of hexaaluminates for catalytic combustion of methane.

2. Experimental

2.1. Preparation of hexaaluminate samples

Hexaaluminate samples were prepared by the urea combustion method using metal nitrate salts as metal cation precursors, and urea $CO(NH_2)_2$ as fuel. Herein, the molar ratio of urea to the total metal ions in hexaaluminates was named R. Stoichiometric amounts of the desired metal nitrates with ions ratio of metal cations and an amount of urea were mixed. The amount of urea was determinated by the value of R. The mixture was mulled at room temperature for about 10 min, and then combusted in a muffle furnace at certain temperature in air. After a few minutes, the combustion reaction was completed and hexaaluminate was obtained. For $LaAl_{12}O_{19}$ and $LaFeAl_{11}O_{19}$ samples, the combustion temperature is in range of 300–800 °C, and for $LaMnAl_{11}O_{19}$ samples, the combustion temperature is in range of 275–800 °C. For the three samples above, the combustion time is 40–60 min, and the R is 1–7. The main aim is to find the optimal preparation conditions of the hexaaluminates. For $AAl_{12}O_{19}$ (A = Sr, Ba, Ca, Ce), $LaMAl_{11}O_{19}$ (M = Cu, Ni, Mg), $SrMAl_{11}O_{19}$ (M = Cu, Mn, Fe, Ni, Mg) and $Sr_{1-x}La_xMnAl_{11}O_{19}$($x$ = 0.2–0.8) hexaaluminates, the preparation conditions are as follows: the combustion temperature is 500 °C, the R is 3, and the combustion time is 40 min.

2.2. Characterization of hexaaluminate samples

The phase structure of the samples was characterized by XRD using a Rigaku D/Max 2500 VB2+/PC diffractometer with a Cu Kα radiation operating at 200 mA and 40 kV. The morphology of the samples was observed by a Hitachi S-4700 field emission scanning electron microscope (SEM). BET specific surface areas (SSA) were determined by nitrogen adsorption at liquid nitrogen temperature, with a Thermo Electron Corporation Sorptomatic 1990 instrument. Prior to each analysis the sample was degassed 4 h at 250 °C under vacuum.

Temperature-programmed reduction (TPR) experiments were performed over 50 mg of sample using a Thermo Electron Corporation TPD/R/O 1100 series Catalytic Surfaces Analyzer equipped with a TC detector. Samples were preheated with 10 vol.% O_2/He mixture heating 20 °C/min up to 400 °C, and then cooling in flowing N_2 down to room temperature, and thereafter reduced with 5 vol.% H_2/N_2 mixture heating 10 °C/min up to 1000 °C. Water produced by the sample reduction was condensed in a cold trap before reaching the detectors. Only H_2 was detected in the outlet gas confirming the effectiveness of the cold trap.

2.3. Catalytic activity tests

Methane catalytic combustion experiments were performed with a conventional fixed-bed quartz reactor (i.d., 8 mm; length, 300 mm) loaded with 0.2 g of the catalysts with a size of 40–60 meshes at atmospheric pressure. Methane combustion involved a gas mixture of 2 vol.% CH_4 in air, with a GHSV of 3000 ml/(g h). The total flow rate in the catalytic test is 10 ml/min. The reaction of methane combustion was stabilized for 30 min at the required temperature, and the outlet products were measured with gas chromatography (Beijing East & West Electronics Institute, GC-4000A). Then, the reaction temperature was increased by 50 °C and the procedure was repeated until methane conversion approached 100%. The reaction temperature was controlled with a K-type thermocouple placed in the vicinity of the catalyst bed. In every case, carbon dioxide and water were the only reaction products detected along the whole experiment.

3. Results and discussions

3.1. $AAl_{12}O_{19}$ (A = La, Sr, Ba, Ca, Ce) hexaaluminates

In urea combustion method, the urea/nitrate ratio and the combustion temperature are key factors in the formation of phase structure of materials. It has been found that materials have good phase structure and catalytic performance when the urea/nitrate ratio is equal to about 3 [24,31]. Combustion is a quick reaction, and products by urea combustion method can be obtained in a short time. Therefore, the combustion time is considered to be a minor factor in the formation of phase structure of materials. However, In order to obtain pure and well-crystallized materials and burn-off any carbonaceous residues, the products are needed to be

kept for a period of time at combustion temperature, or be further calcined at a temperature for a period of time. The period of time varies from minutes to hours [28–30,34]. Herein, when the urea combustion method is used for preparation of $LaAl_{12}O_{19}$ hexaaluminate, the combustion time is 60 min and the value of *R* is 3. The aim is to study the influence of the combustion temperature on the formation of phase structure of $LaAl_{12}O_{19}$. Fig. S1 in the supplementary data shows the XRD spectra of $LaAl_{12}O_{19}$ samples prepared at different combustion temperature.

As shown in Fig. S1, there are not any diffraction peaks when the combustion temperature is 300°C (Fig. S1a), suggesting that there is no formation of the hexaaluminate. When the combustion temperature is 350 °C, the diffraction peaks of $LaAl_{12}O_{19}$ can be observed (Fig. S1b), but the intensity of these peaks is extremely weak, indicating that the phase structure of $LaAl_{12}O_{19}$ starts to be formed. With the combustion temperature increasing up to 400 °C, the intensity of the hexaaluminate diffraction peaks also increases (Fig. S1c). When the combustion temperature further increases up to 500 °C, the intensity of the diffraction peaks increases markedly (Fig. S1d). The characteristic diffraction peaks of $LaAl_{12}O_{19}$ are at 35.9°, 33.8° and 31.9°, respectively, which belong to the magnetoplumbite-type structure. However, when the combustion temperature increases from 500 to 800 °C, the intensity of the diffraction peaks remains almost unchanged. It is indicated that the formation of hexaaluminate structure has completed at 500 °C. In order to check the thermal stability of the sample, the $LaAl_{12}O_{19}$ prepared has been further calcined at 1200 °C for 5 h in air, and its XRD spectra is shown in Fig. S1h. It is found that after the calcination the XRD patterns of this sample keeps almost unchanged, indicating that the hexaaluminate structure is extremely stable. At the same time, no diffraction peaks of other phase structure appear which a pure hexaaluminate can be obtained by the urea combustion method.

Form the above results, $LaAl_{12}O_{19}$ with a pure and complete hexaaluminate structure can be obtained successfully only at 500 °C via the urea combustion method. However, hexaaluminates can be obtained at about 1200 °C by the conventional preparation method reported in literatures. Therefore, the formation of $LaAl_{12}O_{19}$ via the urea combustion method requires much lower temperature in comparison with the conventional preparation methods. During the experiments, the effect of the combustion time on the formation of $LaAl_{12}O_{19}$ has also been investigated. The results show that $LaAl_{12}O_{19}$ with complete hexaaluminate structure can be obtained when the combustion time is equal to about 40 min. When the combustion time further increases, the influence of the combustion time on the formation of phase structure of $LaAl_{12}O_{19}$ is hardly observed. However, the hexaaluminate preparation methods reported in literatures require a long calcination time (about 5 h). Therefore, the urea combustion method used to prepare $LaAl_{12}O_{19}$ requires much less time. Herein, according to the preparation of $LaAl_{12}O_{19}$, a series of $AAl_{12}O_{19}$ (A = Ca, Sr, Ba, Ce) have been prepared under the following preparation conditions: the combustion temperature is 500 °C, the value of the *R* is 3 and the combustion time is 40 min. The XRD patterns of $AAl_{12}O_{19}$ (A = Ca, Sr, Ba, Ce) samples are shown in Fig. 1.

From Fig. 1, all the samples have a pure and complete hexaaluminate structure, suggesting that these hexaaluminates can be prepared successfully under the above conditions. However, the profiles of the diffraction peaks of these hexaaluminates have some changes due to the difference of the cations in A site in $AAl_{12}O_{19}$ (A = Ca, Sr, Ba, Ce). For example, the characteristic diffraction peaks of $AAl_{12}O_{19}$ (A = Ca, Sr, Ce) are basically at 32.2°, 34.2° and 36.2° (JCPDS 38-0470, JCPDS 70-0947, JCPDS 48-0055, Fig. 1a–c), respectively. The three samples exhibit almost the same hexaaluminate crystalline structure, and they belong to the magnetoplumbite-type structure. The characteristic diffraction peaks of $BaAl_{12}O_{19}$ are at 31.9°, 33.0° and 35.6° (JCPDS 26-0135, Fig. 1d), respectively, and it belongs to β-Al_2O_3-type structure. In order to further check the phase stability of hexaaluminate, $LaAl_{12}O_{19}$ has been further calcined at 1500 °C for 5 h in air, and its XRD spectra is shown in Fig. 1e. It is found that after the calcination the small diffraction peaks $LaAlO_3$ in this sample are observed. The specific surface areas of $AAl_{12}O_{19}$ (A = La, Ca, Sr, Ba, Ce) are listed in Table 1. These samples have relatively high specific surface areas varying from 9.1 to 24.3 $m^2\ g^{-1}$. At the same time, after calcination at 1200 °C for 5 h the specific surface area of $LaAl_{12}O_{19}$ keep almost unchanged, suggesting that hexaaluminate materials prepared by the urea combustion method have an excellent thermal stability. In hexaaluminates, mirror planes can be formed by introduction of the large cations (La, Ca, Sr, Ba, Ce), and $Al_2O_4^{2-}$ spinel blocks are separated by these mirror planes, resulting in the fact that the crystal growth along the *c*-axis is suppressed. Therefore, due to this anisotropic crystal shape, a

Table 1
T_{50}, T_{90} and specific surface areas of hexaaluminates

Catalysts	T_{50} (°C)	T_{90} (°C)	S_{BET} ($m^2\ g^{-1}$)
$LaAl_{12}O_{19}$	517	610	9.1
$LaAl_{12}O_{19}$ (1200 °C for 5 h)	519	606	9.4
$SrAl_{12}O_{19}$	529	634	16.0
$BaAl_{12}O_{19}$	543	652	10.6
$CaAl_{12}O_{19}$	550	660	24.3
$CeAl_{12}O_{19}$	574	664	13.9
$LaCuAl_{11}O_{19}$	448	533	19.8
$LaMnAl_{11}O_{19}$	485	567	17.8
$LaMnAl_{11}O_{19}$ (1200 °C for 5 h)	488	570	17.3
$LaFeAl_{11}O_{19}$	512	593	14.2
$LaFeAl_{11}O_{19}$ (1200 °C for 5 h)	513	598	15.0
$LaNiAl_{11}O_{19}$	545	608	11.2
$LaMgAl_{11}O_{19}$	610	684	21.6
$SrCuAl_{11}O_{19}$	457	542	17.1
$SrMnAl_{11}O_{19}$	533	600	15.4
$SrFeAl_{11}O_{19}$	570	640	11.6
$SrNiAl_{11}O_{19}$	587	682	8.7
$SrMgAl_{11}O_{19}$	603	695	18.3
$Sr_{0.2}La_{0.8}MnAl_{11}O_{19}$[a]	514	598	–
$Sr_{0.2}La_{0.8}MnAl_{11}O_{19}$	485	570	18.5
$Sr_{0.4}La_{0.6}MnAl_{11}O_{19}$	490	573	17.7
$Sr_{0.6}La_{0.4}MnAl_{11}O_{19}$	495	577	16.3
$Sr_{0.8}La_{0.2}MnAl_{11}O_{19}$	509	594	18.5

[a] This sample is prepared by co-precipitation method.

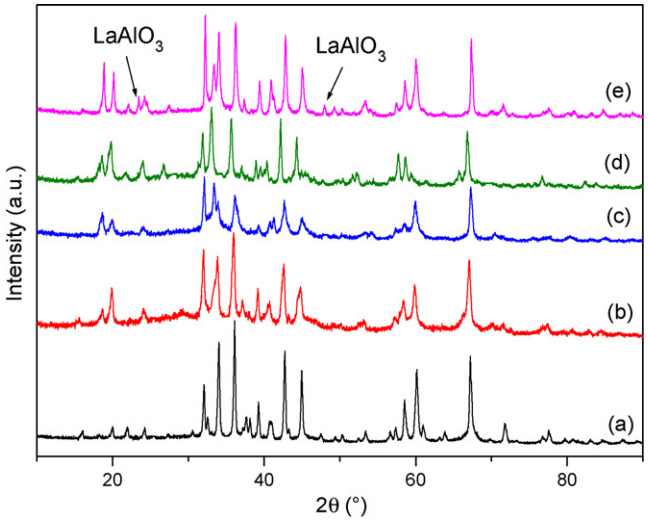

Fig. 1. XRD patterns of $AAl_{12}O_{19}$ (A = Ca, Sr, Ce, Ba) samples: (a) $CaAl_{12}O_{19}$; (b) $SrAl_{12}O_{19}$; (c) $CeAl_{12}O_{19}$; (d) $BaAl_{12}O_{19}$; (e) $LaAl_{12}O_{19}$ (1500 °C and 5 h).

large specific surface area can be maintained at high temperature [39].

3.2. $AMAl_{11}O_{19}$ (A = La, Sr; M = Cu, Mn, Fe, Ni, Mg) hexaaluminates

It has been reported that the partial cation substitution by some transition metals (Co, Ni, Cr, Fe and Mn) for the Al site in hexaaluminate lattice can increase markedly catalytic activity for the combustion of methane [40]. Hence, according to the preparation of $AAl_{12}O_{19}$ (A = La, Ca, Sr, Ba, Ce), we have prepared $LaFeAl_{11}O_{19}$ sample, and the preparation conditions are as follows: the *R* is 3, and the combustion time is 40 min. The aim is to find an optimal combustion temperature. The XRD patterns of $LaFeAl_{11}O_{19}$ samples prepared at different combustion temperature are shown in Fig. S2 in the supplementary data. From Fig. S2, the diffraction peaks of $LaFeAl_{11}O_{19}$ are not observed when the combustion temperature is 300 °C (Fig. S2a), suggesting that $LaFeAl_{11}O_{19}$ hexaaluminate is not formed. When the combustion temperature increases up to 350 °C, some very weak diffraction peaks of $LaFeAl_{11}O_{19}$ appear (Fig. S2b). It is indicated that the $LaFeAl_{11}O_{19}$ hexaaluminate begins to form. With the combustion temperature increasing further up to 400 °C, the intensity of the diffraction peaks further increases, too (Fig. S2c). When the temperature is increased to 500 °C, the intensity of the diffraction peaks increases dramatically (Fig. S2d). The characteristic diffraction peaks of $LaFeAl_{11}O_{19}$ are at 35.9°, 33.8° and 31.9°, respectively, which belong to magnetoplumbite-type structure. However, when the temperature increases from 500 to 800 °C, the intensity of the diffraction peaks remains almost unchanged. It is indicated that $LaFeAl_{11}O_{19}$ with complete hexaaluminate structure has been formed at 500 °C. Fig. S2h shows XRD spectra of the $LaFeAl_{11}O_{19}$ sample calcined at 1200 °C for 5 h in air. It is found that after the calcination the XRD patterns of this sample keeps almost unchanged, indicating that $LaFeAl_{11}O_{19}$ is very stable. At the same time, no diffraction peaks of other phase structure are observed, suggesting that the $LaFeAl_{11}O_{19}$ has a pure hexaaluminate structure.

When the combustion temperature is 500 °C and the combustion time is 40 min, $LaFeAl_{11}O_{19}$ samples with different *R* have been prepared, and Fig. S3 in the supplementary data shows the XRD patterns of these samples. It is obvious that $LaFeAl_{11}O_{19}$ has not been formed when the *R* is 1 (Fig. S3a). When the *R* is 2, the diffraction peaks of $LaFeAl_{11}O_{19}$ appear, but they are extremely weak, suggesting that $LaFeAl_{11}O_{19}$ begins to form (Fig. S3b). When the *R* increases up to 3, the intensity of diffraction peaks increases markedly (Fig. S3c). However, when the *R* increases from 3 to 7, the intensity of the diffraction peaks remains almost unchanged. It is indicated that $LaFeAl_{11}O_{19}$ with complete structure has been already formed when the *R* is 3. It seems that there is no effect on the formation of $LaFeAl_{11}O_{19}$ when the amount of urea further increases.

From the above results, it is found that $LaFeAl_{11}O_{19}$ hexaaluminate can be prepared by the urea combustion method under the proper preparation conditions. Subsequently, we have prepared $LaMnAl_{11}O_{19}$ hexaaluminate material. Firstly, the influence of the combustion temperature on the formation of $LaMnAl_{11}O_{19}$ is investigated. $LaMnAl_{11}O_{19}$ samples are prepared at different combustion temperature, and other preparation conditions are as follows: the *R* is 3 and the combustion time is 40 min. The XRD patterns of these samples are shown in Fig. S4 in the supplementary data. Obviously, when the combustion temperature is 275 °C, there are not diffraction peaks (Fig. S4a). When the combustion temperature increases to 300 °C, the very weak diffraction peaks of $LaMnAl_{11}O_{19}$ appear, suggesting that $LaMnAl_{11}O_{19}$ begins to form at 300 °C (Fig. S4b). With the combustion temperature increasing up to 350 °C, the intensity of the diffraction peaks increases (Fig. S4c). When the temperature further increases up to 400 °C, the intensity of the diffraction peaks increases markedly (Fig. S4d). The characteristic diffraction peaks are at 35.9°, 33.8° and 31.9°, respectively (JCPDS 36-1217), which belongs to the maguetoplumbite-type structure. However, when the combustion temperature increases from 400 to 800 °C, the intensity of diffraction peaks of $LaMnAl_{11}O_{19}$ keeps almost unchanged, suggesting that $LaMnAl_{11}O_{19}$ has been formed completely at 400 °C. Fig. S4i shows XRD spectra of the $LaMnAl_{11}O_{19}$ sample calcined at 1200 °C for 5 h in air. It is found that after the calcination the XRD patterns of this sample keeps almost unchanged, indicating that $LaMnAl_{11}O_{19}$ has an excellent thermal stability. In addition, no other phase structure appears.

Secondly, the influence of the amount of urea on the formation of $LaMnAl_{11}O_{19}$ has been studied. $LaMnAl_{11}O_{19}$ samples have been prepared at different *R* when the combustion temperature is 400 °C and the combustion time is 40 min. Their XRD patterns are shown in Fig. S5 in the supplementary data. It is found that there are not any diffraction peaks when the *R* is 1 (Fig. S5a). When the *R* is 2, the diffraction peaks of $LaMnAl_{11}O_{19}$ appear, suggesting that $LaMnAl_{11}O_{19}$ begins to form (Fig. S5b). When the *R* increases up to 3, the intensity of these diffraction peaks increases dramatically (Fig. S5c). However, when the amount of urea further increases, the intensity of these diffraction peaks remains almost unchanged. It is indicated that $LaMnAl_{11}O_{19}$ with complete structure has been formed when the *R* is 3, and the further increase of the amount of urea has no effect on the formation of $LaMnAl_{11}O_{19}$.

The influences of the combustion temperature and the value of *R* on the formation of $LaFeAl_{11}O_{19}$ and $LaMnAl_{11}O_{19}$ have been investigated. The two hexaaluminates with a pure and complete structure can be obtained at proper preparation conditions. For $LaFeAl_{11}O_{19}$, the proper preparation conditions are as follows: the combustion temperature is not less than 500 °C, the value of *R* is in the range 3–7, and the combustion time is 40 min. For $LaMnAl_{11}O_{19}$, the proper preparation conditions are as follows: the combustion temperature is not less than 400 °C, the value of *R* is in the range 3–7, and the combustion time is 40 min. Considering the preparation conditions, the influence of the amount of urea on the formation of the two samples is almost the same, and they can be obtained when the *R* is 3–7. However, their combustion temperature is different, and the formation of $LaFeAl_{11}O_{19}$ requires higher combustion temperature than that of $LaMnAl_{11}O_{19}$ does, suggesting that introduction of Mn can improve the formation of $LaMnAl_{11}O_{19}$ [15].

According to the preparation of the above two samples, we have prepared $LaMAl_{11}O_{19}$ (M = Cu, Ni, Mg) and $SrMAl_{11}O_{19}$ (M = Cu, Mn, Fe, Ni, Mg) hexaaluminates. The preparation conditions are as follows: the combustion temperature is 500 °C, the value of *R* is 3, and the combustion time is 40 min. The XRD patterns of these samples are shown in Figs. 2 and 3. From Fig. 2, it is found that all samples have complete phase structure of hexaaluminate. For $LaMAl_{11}O_{19}$ (M = Ni, Mg) samples (Fig. 2a and b), their characteristic diffraction peaks are basically at 31.9°, 33.8° and 35.9°, respectively, belonging to the magnetoplumbite-type structure. The characteristic diffraction peaks of $LaCuAl_{11}O_{19}$ (Fig. 2c) are slightly shifted compared to the patterns of the above two samples. The main reason is that the partial substitution of Cu leads to a cell expansion due to the larger size of Cu^{2+} ions compared to that of Al^{3+} ions [41]. At the same time, the intensity of the diffraction peaks of these samples is different with the different B site ions. For example, the intensity of the diffraction peaks is weakest in these samples when the Cu ions are at B site. In order to check the phase stability of hexaaluminate, $LaFeAl_{11}O_{19}$ and $LaMnAl_{11}O_{19}$ have been further calcined at 1500 °C for 5 h in air, and its XRD spectra is shown in Fig. 2d and e. It is found that after the calcination there is no other phase in the $LaFeAl_{11}O_{19}$ sample, whereas there is a diffraction peak of $LaAlO_3$ in the $LaMnAl_{11}O_{19}$ sample. From Fig. 3, it is found that $SrMAl_{11}O_{19}$

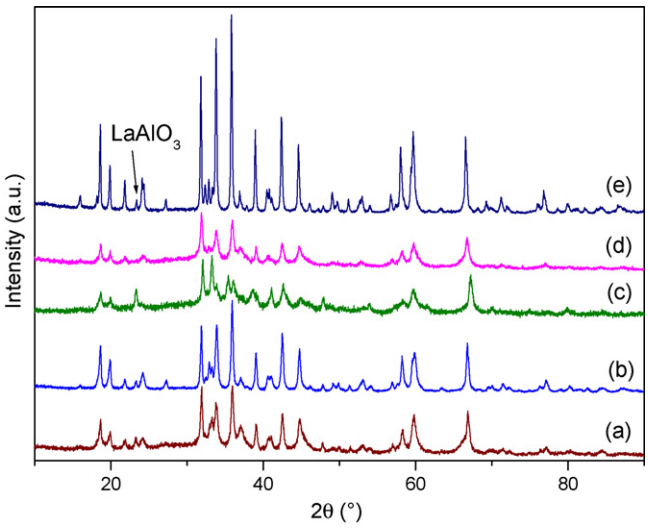

Fig. 2. XRD patterns of $LaMAl_{11}O_{19}$ (M = Ni, Mg, Cu) samples: (a) $LaNiAl_{11}O_{19}$; (b) $LaMgAl_{11}O_{19}$; (c) $LaCuAl_{11}O_{19}$; (d) $LaFeAl_{11}O_{19}$ (1500 °C and 5 h); (e) $LaMnAl_{11}O_{19}$ (1500 °C and 5 h).

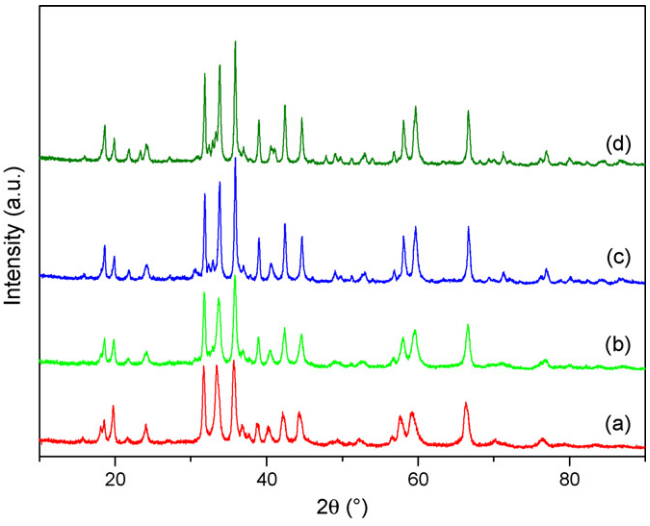

Fig. 4. XRD patterns of $Sr_{1-x}La_xMnAl_{11}O_{19}$ samples: (a) $Sr_{0.8}La_{0.2}MnAl_{11}O_{19}$; (b) $Sr_{0.6}La_{0.4}MnAl_{11}O_{19}$; (c) $Sr_{0.4}La_{0.6}MnAl_{11}O_{19}$; (d) $Sr_{0.2}La_{0.8}MnAl_{11}O_{19}$.

(M = Cu, Mn, Fe, Ni, Mg) samples have a pure and complete phase structure of hexaaluminate. Their characteristic diffraction peaks are basically at 31.9°, 33.8° and 35.9°, respectively. These samples belong to the magnetoplumbite-type structure. Similarly, the intensity of the diffraction peaks of these samples is different with various B site ions. For example, $SrFeAl_{11}O_{19}$ and $SrCuAl_{11}O_{19}$ have weaker diffraction peaks in these samples.

The SSA of $AMAl_{11}O_{19}$ (A = La, Sr; M = Cu, Mn, Fe, Ni, Mg) samples are shown in Table 1. These hexaaluminates have relatively high specific surface areas. The SSAs of $LaMAl_{11}O_{19}$ (M = Cu, Mn, Fe, Ni, Mg) samples vary from 11.2 to 21.6 $m^2\,g^{-1}$, and the SSAs of $SrMAl_{11}O_{19}$ (M = Cu, Mn, Fe, Ni, Mg) samples are in the range 8.7–18.3 $m^2\,g^{-1}$. It is clear that for those samples with the same M ions, La-based hexaaluminate samples have higher specific surface areas than Sr-based hexaaluminate samples. The main reason is likely that the ionic radii of La^{3+} (0.106 nm) is smaller than that of Sr^{2+} (0.120 nm), and the migration of La^{3+} into the lattice of γ-Al_2O_3 is easier than that of Sr^{3+}. Accordingly, the La-based hexaaluminates can be formed at lower temperature than the Sr-based

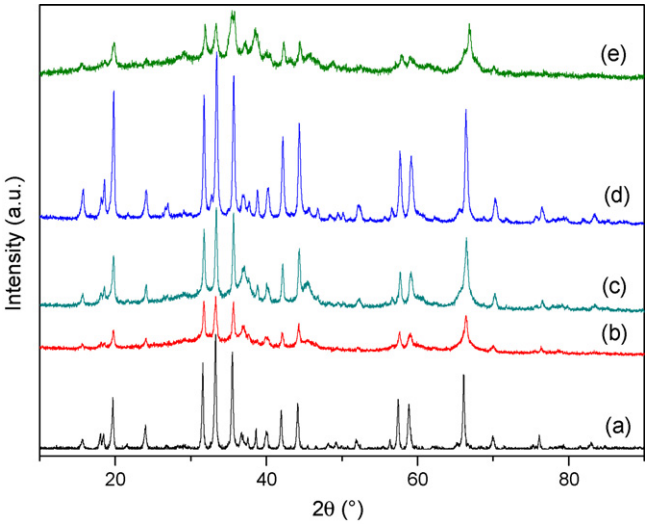

Fig. 3. XRD patterns of $SrMAl_{11}O_{19}$ (M = Mn, Fe, Ni, Mg, Cu) samples: (a) $SrMnAl_{11}O_{19}$; (b) $SrFeAl_{11}O_{19}$; (c) $SrNiAl_{11}O_{19}$; (d) $SrMgAl_{11}O_{19}$; (e) $SrCuAl_{11}O_{19}$.

samples, which suppresses the phase transition from γ-Al_2O_3 to α-Al_2O_3 maintaining relatively high specific surface areas. The study by Groppi et al. [7] also shows that La^{3+} used as mirror plane cations can not only improve the stability but also maintain the relatively high specific surface areas of hexaaluminate materials. At the same time, after calcination at 1200 °C for 5 h the specific surface areas of $LaAl_{12}O_{19}$ and $LaMnAl_{11}O_{19}$ samples keep almost unchanged, suggesting that hexaaluminate materials prepared by the urea combustion method have an excellent thermal stability.

3.3. $Sr_{1-x}La_xMnAl_{11}O_{19}$ (x = 0.2–0.8) hexaaluminates

It has been extensively reported that $Sr_{1-x}La_xMnAl_{11}O_{19}$ hexaaluminates have excellent catalytic activity and thermal stability for combustion of methane [5,42–44]. Herein, a series of $Sr_{1-x}La_xMnAl_{11}O_{19}$ hexaaluminate materials (x = 0.2–0.8) have been prepared via the urea combustion method. According to the previous preparation of hexaaluminates, the preparation conditions are as follows: the combustion temperature is 500 °C, the R is 3 and the combustion time is 40 min. Fig. 4 shows the XRD patterns of $Sr_{1-x}La_xMnAl_{11}O_{19}$ (x = 0.2–0.8) samples. It is clear that all the samples have a pure and complete phase structure of hexaaluminate. The series of samples exhibit almost the same hexaaluminate crystalline structure; their characteristic diffraction peaks are basically at 31.9°, 33.8°, and 35.9°, respectively, belonging to the magnetoplumbite-type structure. However, there is still a slight shift in 2θ of the diffraction peaks due to the difference of the ratio of La to Sr. The main reason is likely that introduction of different ions in hexaaluminates leads to different lattice deformation.

The specific surface areas of $Sr_{1-x}La_xMnAl_{11}O_{19}$ (x = 0.2–0.8) are shown in Table 1. These samples have relatively high specific surface areas varying from 16.3 to 18.5 $m^2\,g^{-1}$. At the same time, form Table 1, the specific surface area of $SrMnAl_{11}O_{19}$ is lower than that of $Sr_{1-x}La_xMnAl_{11}O_{19}$ (x = 0.2–0.8), suggesting that introduction of La in hexaaluminates can improve the specific surface areas of these samples [7].

3.4. Surface morphology of hexaaluminates

The surface morphology of $LaAl_{12}O_{19}$, $LaFeAl_{11}O_{19}$ and $LaMnAl_{11}O_{19}$ is shown in Fig. 5. The preparation conditions of

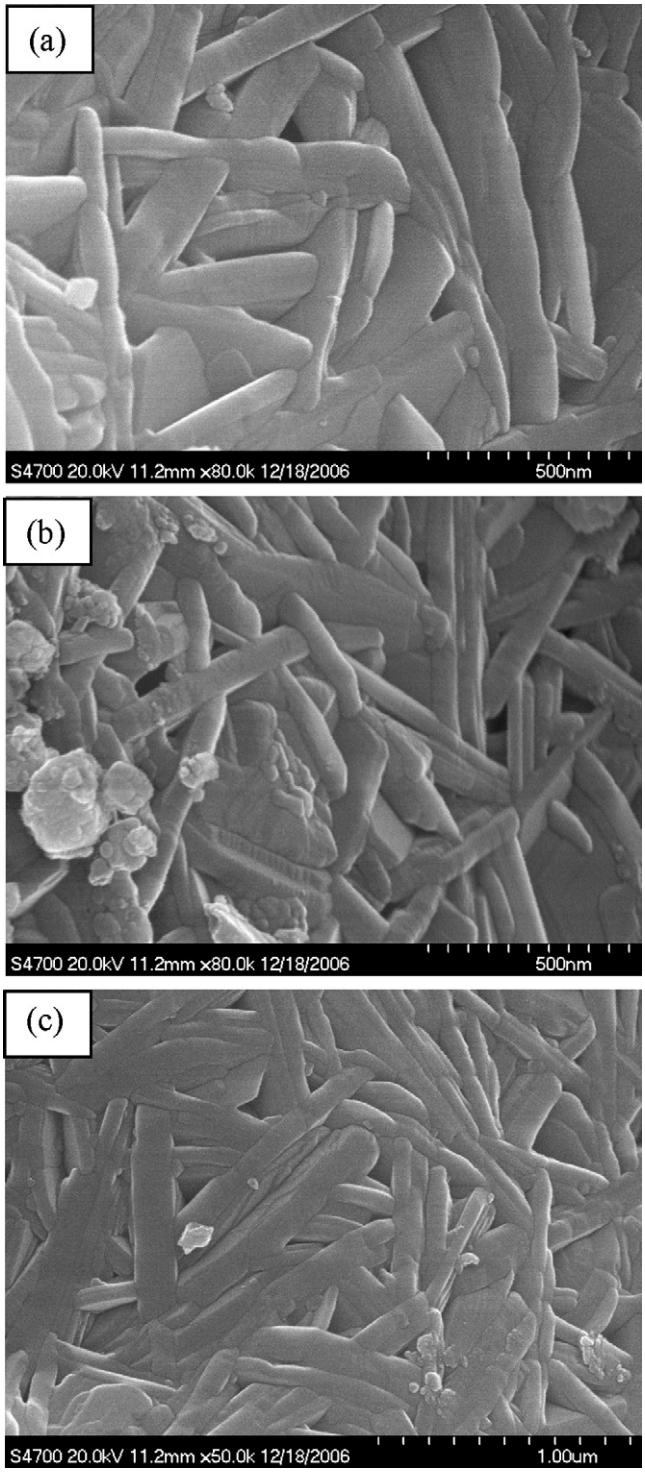

Fig. 5. Surface morphology of hexaaluminate samples: (a) $LaAl_{12}O_{19}$; (b) $LaFeAl_{11}O_{19}$; (c) $LaMnAl_{11}O_{19}$.

$LaAl_{12}O_{19}$ and $LaFeAl_{11}O_{19}$ are as follows: the combustion temperature is 500 °C, the value of the *R* is 3 and the combustion time is 40 min. The preparation conditions of $LaMnAl_{11}O_{19}$ are as follows: the combustion temperature is 400 °C, the value of the *R* is 3 and the combustion time is 40 min. From Fig. 5, it is found that the samples have a plate-like morphology, which is the characteristic morphology of hexaaluminate. It is indicated that these hexaaluminates has been formed at the preparation conditions. The plate-like

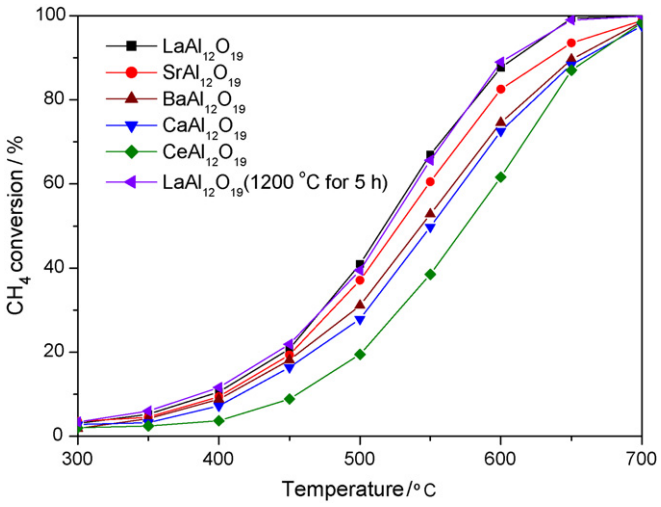

Fig. 6. Catalytic activity of $AAl_{12}O_{19}$ (A = La, Sr, Ba, Ca, Ce) samples.

morphology of hexaaluminate is obtained through the anisotropic crystal growth, which is typical for the excellent combustion catalyst at high temperature. The kind of morphology can maintains high the specific surface area and improves the thermal stability of hexaaluminate materials [45].

3.5. Catalytic activity of hexaaluminates

For comparison, the preparation conditions of the samples for catalytic activity tests are the same, and as follows: the combustion temperature is 500 °C, the *R* is 3, and the combustion time is 40 min. The temperature required for a 50% conversion of CH_4 (T_{50}) and the temperature required for a 90% conversion of CH_4 (T_{90}) are used to evaluate the activity for methane combustion, and T_{50} and T_{90} are listed in Table 1. Fig. 6 shows the results of catalytic activity of $AAl_{12}O_{19}$ (A = La, Sr, Ba, Ca, Ce) hexaaluminates. The results of catalytic activity of $LaAl_{12}O_{19}$ calcined at 1200 °C for 5 h are also shown in Fig. 6, and its T_{50} and T_{90} are also listed in Table 1. It is found that activities of the hexaaluminates are different with various A site ions. In these catalysts, $LaAl_{12}O_{19}$ catalyst exhibits the best activity for combustion of methane. After calcinations at 1200 °C for 5 h, the activity of $LaAl_{12}O_{19}$ remains almost unchanged, indicating that the hexaaluminate material has an excellent stability. $CeAl_{12}O_{19}$ catalyst shows the lowest activity. The order of activities of these catalysts is $LaAl_{12}O_{19} > SrAl_{12}O_{19} > BaAl_{12}O_{19} > CaAl_{12}O_{19} > CeAl_{12}O_{19}$. It was reported that the T_{10} of $LaAl_{12}O_{19}$ and $BaAl_{12}O_{19}$ prepared by co-precipitation method was about 650 °C when reactant gas was 1 vol.% methane in air with a GHSV of 70,000 $cm^3/(g\,h)$ [5]. Artizzu et al. [41] prepared $BaAl_{12}O_{19}$ for catalytic combustion of methane by alkoxide hydrolysis method. When the reactant gas mixture consisted of 1 vol.% CH_4, 4 vol.% O_2 and 95% N_2, the T_{50} and T_{90} of the catalyst were 765 and 780 °C, respectively, under a GHSV of 15,000 h^{-1}.

The catalytic activities of $LaMAl_{11}O_{19}$ (M = Cu, Mn, Fe, Ni, Mg) and $SrMAl_{11}O_{19}$ (M = Cu, Mn, Fe, Ni, Mg) hexaaluminates are shown in Figs. 12 and 13, respectively. The results of catalytic activity of $LaFeAl_{11}O_{19}$ and $LaMnAl_{11}O_{19}$ calcined at 1200 °C for 5 h are also shown in Fig. 7, and its T_{50} and T_{90} are also listed in Table 1. As shown in Fig. 7, their activities are different with various M ions. $LaCuAl_{11}O_{19}$ catalyst exhibits the best catalytic activity. $LaMgAl_{11}O_{19}$ catalyst has the lowest catalytic activity. After calcinations at 1200 °C for 5 h, the activities of $LaFeAl_{11}O_{19}$ and $LaMnAl_{11}O_{19}$ remain almost

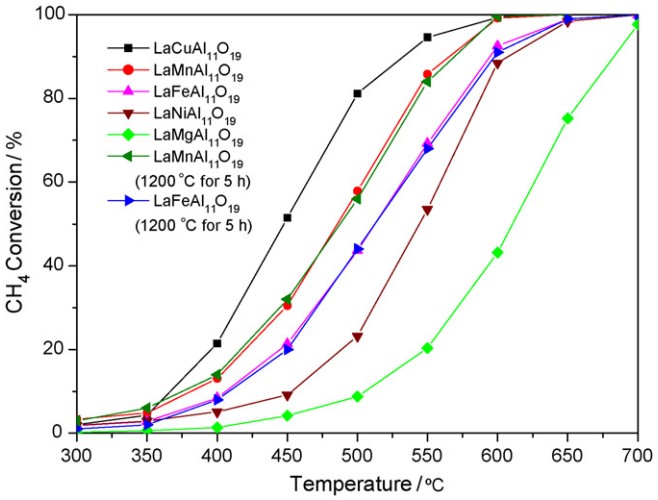

Fig. 7. Catalytic activity of $LaMAl_{11}O_{19}$ (M = Cu, Mn, Fe, Ni, Mg) samples.

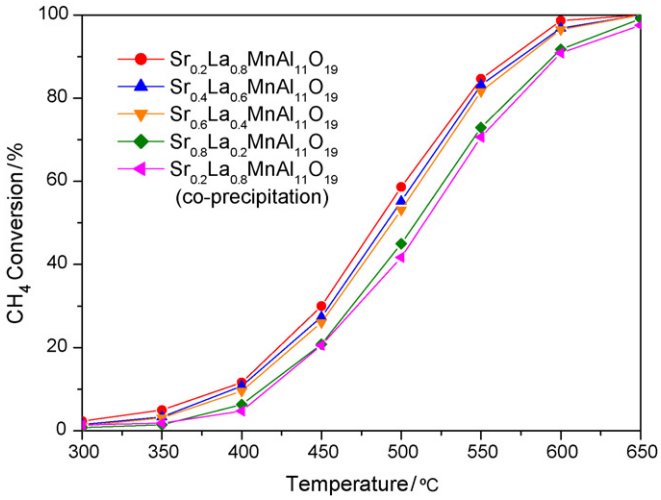

Fig. 9. Catalytic activity of $Sr_{1-x}La_xMnAl_{11}O_{19}$ (x = 0–1) samples.

unchanged, indicating that the hexaaluminate materials have an excellent stability. The order of activity of these catalysts is $LaCuAl_{11}O_{19} > LaMnAl_{11}O_{19} > LaFeAl_{11}O_{19} > LaNiAl_{11}O_{19} > LaMgAl_{11}O_{19}$. Ersson et al. [46] prepared $LaMnAl_{11}O_{19}$ catalyst by co-precipitation method. When GHSV was 100,000 h^{-1} and a methane concentration of 1.5 mol% was used, the temperature for 20% conversion of methane was 715 °C. Li et al. [47] prepared $LaMnAl_{11}O_{19}$ catalyst for catalytic combustion of methane using the same method. When the reactant gas was 4 vol.% O_2 and 1 vol.% CH_4 (nitrogen as balance) and GHSV = 15,000 h^{-1}, the T_{50} and T_{90} were 690 and 820 °C, respectively. When the A site ion is Sr, as shown in Fig. 8, these samples also show excellent activity for combustion of methane. In these catalysts, the order of activity is $SrCuAl_{11}O_{19} > SrMnAl_{11}O_{19} > SrFeAl_{11}O_{19} > SrNiAl_{11}O_{19} > SrMgAl_{11}O_{19}$, which is the same as that of $LaMAl_{11}O_{19}$ (M = Cu, Mn, Fe, Ni, Mg) catalysts. Inoue et al. [10] prepared $SrMnAl_{11}O_{19}$ catalyst for methane combustion using alkoxide hydrolysis method. When the reactant gas was 1 vol.% CH_4 in air with a flow rate of 48,000 $cm^3\ h^{-1}$, the T_{10} and T_{90} of this catalyst were 550 and 770 °C, respectively. The catalytic activities of $Sr_{1-x}La_xMnAl_{11}O_{19}$ (x = 0–1) catalysts are shown in Fig. 9. It is found that $LaMnAl_{11}O_{19}$ catalyst exhibits good activity, and the activity decreases when the Sr is added. Moreover, the activities of these catalysts decrease gradually with increasing of the Sr content in $Sr_{1-x}La_xMnAl_{11}O_{19}$. However, when the Sr content increases from 0 to 0.6, the decrease extent of activity of these samples is extremely small. In other words, their catalytic activities are very close. When the Sr content increases from 0.6 to 0.8, the decrease extent of activity of these catalysts becomes large again. Obviously, $SrMnAl_{11}O_{19}$ catalyst shows the lowest activity. From the results above, when La is introduced to $SrMnAl_{11}O_{19}$, the activities of catalysts increases markedly, suggesting that La component in catalysts plays an important role to the catalytic activity for combustion of methane. Machida et al. [43] prepared a series of $Sr_{1-x}La_xMnAl_{11}O_{19}$ (x = 0–0.8) hexaaluminates for catalytic combustion of methane by an alkoxide hydrolysis method, and found that $Sr_{0.8}La_{0.2}MnAl_{11}O_{19}$ catalyst had the best activity in these catalysts, which was different from our experimental results. The main reason is likely that the preparation method is different. Yeh et al. [48] prepared $Sr_{0.8}La_{0.2}MnAl_{11}O_{19}$ catalyst for catalytic combustion of methane using co-precipitation method. When the reactant gas was 1 vol.% in air and GHSV was 48,000 h^{-1}, the T_{50} and T_{90} of the catalyst calcined at 1200 °C with 20 $m^2\ g^{-1}$ were 639 and 735 °C, respectively.

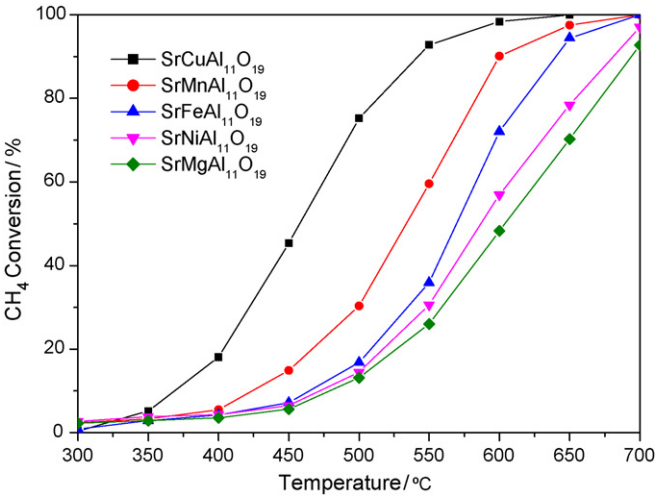

Fig. 8. Catalytic activity of $SrMAl_{11}O_{19}$ (M = Cu, Mn, Fe, Ni, Mg) samples.

From Table 1, it is found that for $AAl_{12}O_{19}$ (A = La, Sr, Ba, Ca, Ce), $AMAl_{11}O_{19}$ (A = La, Sr; M = Cu, Mn, Fe, Ni, Mg) and $Sr_{1-x}La_xMnAl_{11}O_{19}$ (x = 0.2–0.8) hexaaluminate catalysts, the order of activity of these catalysts is not related to their corresponding specific surface areas, suggesting that the specific surface area of catalysts is not main factor in activities.

3.6. Temperature-programmed reduction measurements

In order to further investigate the relationship between the structure and performance of these hexaaluminate catalysts, the H_2-TPR of these catalysts are measured, and the H_2-TPR profiles are shown in Figs. 10–13, respectively. From Table 1, methane can be totally converted into CO_2 and H_2O below 700 °C over these catalysts. Therefore, the redox properties below 700 °C have a significant effect on the catalytic activity of catalysts.

Fig. 10 shows the H_2-TPR profiles of $AAl_{12}O_{19}$ (A = La, Sr, Ba, Ca, Ce) hexaaluminates. It is found that the H_2-TPR profiles of these catalysts are different with various A site ions, which is related not only to the nature of A site ions but also to the interaction between the A site ions and other adjacent ions. Because the thickness of the mirror planes depends on the A site ions, the oxygen diffusion in hexaaluminates with different A site ions is different. Therefore, the H_2-TPR profiles of these catalysts are different from each other due

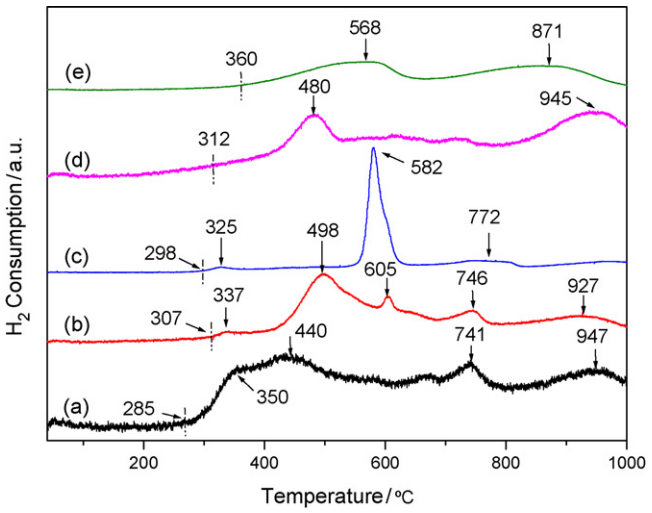

Fig. 10. H_2-TPR profiles of $AAl_{12}O_{19}$ (A = La, Sr, Ba, Ca, Ce) samples: (a) $LaAl_{12}O_{19}$; (b) $SrAl_{12}O_{19}$; (c) $BaAl_{12}O_{19}$; (d) $CaAl_{12}O_{19}$; (e) $CeAl_{12}O_{19}$.

to the difference of A site ions. For $LaAl_{12}O_{19}$ catalyst, the reduction peak begins at 285 °C, namely, the initial reduction temperature is 285 °C. At the same time, there are four reduction peaks at 350, 440, 741 and 947 °C, respectively, indicating that there are four oxygen species in $LaAl_{12}O_{19}$ catalyst (Fig. 10a). In these catalysts, $LaAl_{12}O_{19}$ catalyst has the lowest initial reduction temperature and the largest reduction peak area below 700 °C. Therefore, this catalyst exhibits the best catalytic activity for combustion of methane. In the case of $SrAl_{12}O_{19}$ catalyst, the initial reduction temperature is 307 °C, and there are five reduction peaks at 337, 498, 605, 746 and 927 °C, respectively (Fig. 10b). In comparison with $LaAl_{12}O_{19}$ catalyst, the initial reduction temperature of $SrAl_{12}O_{19}$ catalyst increases, temperature of the main reduction peak (at 498 °C) increases and the main reduction peak area decreases, suggesting that the catalytic activity of $SrAl_{12}O_{19}$ catalyst decreases. $BaAl_{12}O_{19}$ catalyst begins to be reduced at 298 °C, and there are three reduction peaks at 325, 582 and 772 °C, respectively (Fig. 10c). Chu et al. [49] prepared $BaAl_{12}O_{19}$ hexaaluminate by co-precipitation method, and found that $BaAl_{12}O_{19}$ did not show a reduction peak between 50 and 1050 °C. The main reason is likely that the preparation method is different. In comparison with $SrAl_{12}O_{19}$ catalyst, though the initial reduction temperature of $BaAl_{12}O_{19}$ decreases, the temperature of its main reduction peak (at 582 °C) increases markedly and the main reduction peak area of $BaAl_{12}O_{19}$ catalyst decreases. Therefore, $BaAl_{12}O_{19}$ catalyst has less activity than $SrAl_{12}O_{19}$ catalyst. $CaAl_{12}O_{19}$ catalyst begins to be reduced at 312 °C, and there are a low temperature reduction peak (at 480 °C) and a high temperature reduction peak (945 °C) (Fig. 10d). In comparison with $BaAl_{12}O_{19}$ catalyst, the initial reduction temperature of $CaAl_{12}O_{19}$ catalyst increases slightly. Though the temperature of the main reduction peak (at 480 °C) decreases, the main reduction peak area decreases markedly. Therefore, $CaAl_{12}O_{19}$ catalyst shows the less activity. The initial reduction temperature of $CeAl_{12}O_{19}$ is 360 °C, and there are two reduction peaks at 568 and 871 °C, respectively (Fig. 10e). $CeAl_{12}O_{19}$ catalyst has the highest initial reduction temperature and the lowest reduction peak area, resulting in the lowest catalytic activity. From the analysis of H_2-TPR profiles of $AAl_{12}O_{19}$ (A = La, Sr, Ba, Ca, Ce) catalysts, there is a corresponding relationship between the activity and the redox properties of these catalysts.

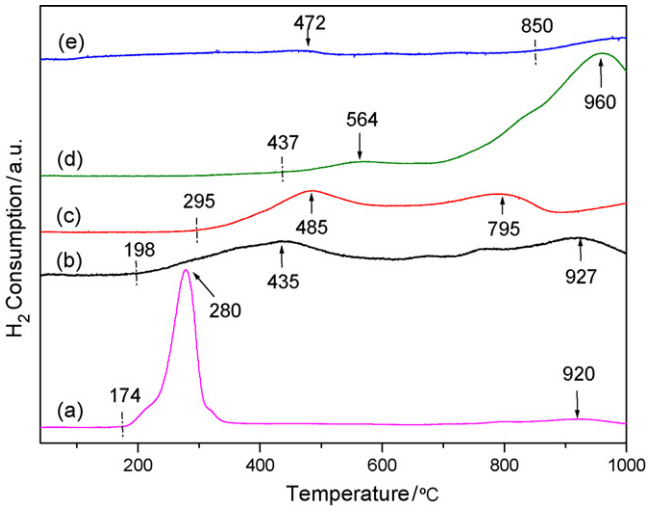

Fig. 11. H_2-TPR profiles of $LaMAl_{11}O_{19}$ (M = Cu, Mn, Fe, Ni, Mg) samples: (a) $LaCuAl_{11}O_{19}$; (b) $LaMnAl_{11}O_{19}$; (c) $LaFeAl_{11}O_{19}$; (d) $LaNiAl_{11}O_{19}$; (e) $LaMgAl_{11}O_{19}$.

The H_2-TPR profiles of $LaMAl_{11}O_{19}$ (M = Cu, Mn, Fe, Ni, Mg) catalysts are shown in Fig. 11. It is clear that the H_2-TPR profiles of these catalysts are different with various M ions. The H_2-TPR profiles of these catalysts are related to the phase structure, the amount of activity component M in surface, the nature of M and the coordinate of M and other adjacent atoms. $LaCuAl_{11}O_{19}$ catalyst begins to be reduced at 174 °Cand there is a large reduction peak at 280 °C (Fig. 11a). It is indicated that Cu^{2+} has a high surface concentration in this catalyst, and is reduced easily. Furthermore, this reduction occurs in a single step without intermediate Cu^{+} formation [41]. At the same time, there is another weak reduction peak at 920 °C, suggesting that there is another oxygen species in this catalyst. In these catalysts, $LaCuAl_{11}O_{19}$ has the lowest initial reduction temperature and the largest reduction peak area. Accordingly, $LaCuAl_{11}O_{19}$ catalyst shows the best catalytic activity. $LaMnAl_{11}O_{19}$ catalyst begins to be reduced at 198 °C, and has two reduction peaks at 435 and 927 °C, respectively (Fig. 11b). It has been reported [7,50,51] that the low temperature reduction peak is attributed to the process of $Mn^{3+} \rightarrow Mn^{2+}$. However, there is no clear attribution to the high temperature reduction peak. In comparison with $LaCuAl_{11}O_{19}$ catalyst, the initial reduction temperature of $LaMnAl_{11}O_{19}$ catalyst increases, its main reduction peak shifts to higher temperature (at 435 °C), and the reduction peak area decreases. So $LaMnAl_{11}O_{19}$ catalyst exhibits lower activity. The initial reduction temperature of $LaFeAl_{11}O_{19}$ catalyst is 295 °C (Fig. 11c), and there are two reduction peaks at 485 and 795 °C, which are attributed to the process of $Fe^{3+} \rightarrow Fe^{2+}$ and $Fe^{2+} \rightarrow Fe^{0}$, respectively [51]. In comparison with $LaMnAl_{11}O_{19}$ catalysts, the initial reduction temperature increases continuously, the main reduction peak shifts to higher temperature (at 485 °C), and the reduction peak area decreases, resulting in decrease of activity of $LaFeAl_{11}O_{19}$ catalyst. $LaNiAl_{11}O_{19}$ catalyst begins to be reduced at 437 °C, and has two reduction peaks at 564 and 960 °C, respectively (Fig. 11d). The high temperature reduction peak belongs to the process of $Ni^{2+} \rightarrow Ni^{0}$ [12,52]. The reduction process of $Ni^{2+} \rightarrow Ni^{0}$ in $LaNiAl_{11}O_{19}$ occurs at such high temperature, indicating that Ni is more strongly bonded in hexaaluminate structure. In comparison with $LaFeAl_{11}O_{19}$ catalyst, the initial reduction temperature further increases, the main reduction peak further increases, and the reduction peak area decreases markedly. Therefore, the catalytic activity of $LaNiAl_{11}O_{19}$ catalyst further decreases. For $LaMgAl_{11}O_{19}$, there is an extremely weak reduction peak at 472 °C, resulting in the lowest activity (Fig. 11e). At the same time, another reduction peak starts to be reduced at about 850 °C, and this peak has not drop down even up to 1000 °C, likely because Mg^{2+} ions in the hexaaluminate lattices are extremely stable and only a part of Mg^{2+} can be reduced to Mg^{0} at 1000 °C, suggesting that Mg ions are more strongly bonded in

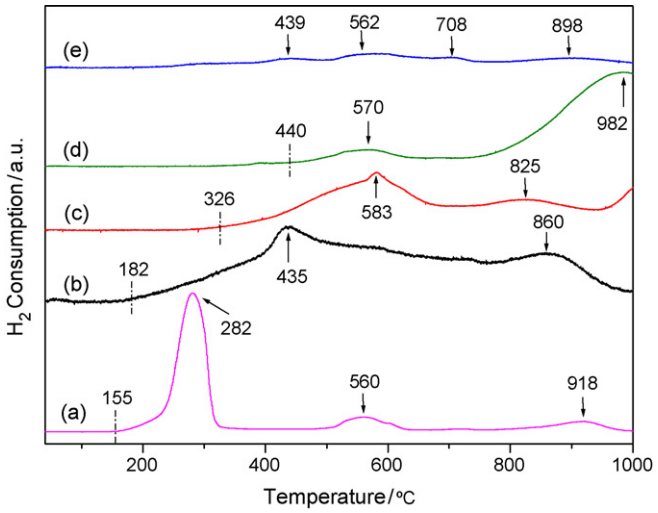

Fig. 12. H_2-TPR profiles of $SrMAl_{11}O_{19}$ (M = Cu, Mn, Fe, Ni, Mg) samples: (a) $SrCuAl_{11}O_{19}$; (b) $SrMnAl_{11}O_{19}$; (c) $SrFeAl_{11}O_{19}$; (d) $SrNiAl_{11}O_{19}$; (e) $SrMgAl_{11}O_{19}$.

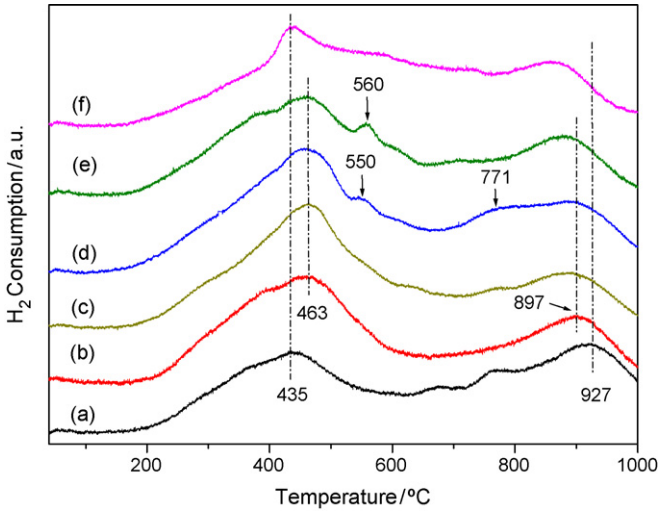

Fig. 13. H_2-TPR profiles of $Sr_{1-x}La_xMnAl_{11}O_{19}$ samples: (a) $LaMnAl_{11}O_{19}$; (b) $Sr_{0.2}La_{0.8}Mn\ Al_{11}O_{19}$; (c) $Sr_{0.4}La_{0.6}Mn\ Al_{11}O_{19}$; (d) $Sr_{0.6}La_{0.4}Mn\ Al_{11}O_{19}$; (e) $Sr_{0.8}La_{0.2}Mn\ Al_{11}O_{19}$; (f) $SrMnAl_{11}O_{19}$.

hexaaluminate lattices. The H_2-TPR profiles of $SrMAl_{11}O_{19}$ (M = Cu, Mn, Fe, Ni, Mg) catalysts are shown in Fig. 12. The H_2-TPR profiles of these catalysts seem to exhibit almost the same reduction profiles in shape as $LaMAl_{11}O_{19}$ (M = Cu, Mn, Fe, Ni, Mg) catalysts, only their reduction temperature is different. $SrCuAl_{11}O_{19}$ catalyst starts to be reduced at 155 °C. Besides a stronger reduction peak at 282 °C, which is attributed to the process of $Cu^{2+} \rightarrow Cu^0$, there are two weak reduction peaks at 560 °C and 918 °C, respectively (Fig. 12a). It is indicated that the H_2-TPR profiles have changed when the A site ion is Sr. $SrMnAl_{11}O_{19}$ catalyst begins to be reduced at 182 °C, and there are a low temperature reduction peak at 435 °C and a high temperature reduction peak at 860 °C (Fig. 12b). For $SrFeAl_{11}O_{19}$ catalyst, the initial reduction temperature is 326 °C, its low temperature reduction peak is at 583 °C and its high temperature reduction peak is at 825 °C (Fig. 12c). For $SrMAl_{11}O_{19}$ (M = Cu, Mn, Fe) catalysts, the order of the initial reduction temperature in terms of M ions is: Cu < Mn < Fe. The temperature of the main reduction peak of these catalysts increases as the same order. However, the reduction peak area decreases gradually as the same order above. Therefore, the order of catalytic activities of the catalysts is $SrCuAl_{11}O_{19} > SrMnAl_{11}O_{19} > SrFeAl_{11}O_{19}$. $SrNiAl_{11}O_{19}$ begins to be reduced at 440 °C, its low temperature reduction peak is at 570 °C, and its high temperature reduction peak is at 982 °C (Fig. 12d). In comparison with $SrFeAl_{11}O_{19}$ catalyst, though the temperature of the reduction peak at 570 °C of $SrNiAl_{11}O_{19}$ catalyst decreases, its reduction peak area decreases markedly. Therefore, the activity of $SrNiAl_{11}O_{19}$ catalyst is lower than that of $SrFeAl_{11}O_{19}$ catalyst. There are four reduction peaks at 439, 562, 708 and 898 °C, respectively (Fig. 12e) and that the H_2-TPR profiles of $SrMgAl_{11}O_{19}$ have changed when the B site ion is Mg in comparison with $LaMgAl_{11}O_{19}$ catalyst. Below 700 °C, the reduction peak area of the reduction peaks over $SrMgAl_{11}O_{19}$ is extremely small. Hence, $SrMgAl_{11}O_{19}$ catalyst shows the lowest catalytic activity. From the results above, $SrMAl_{11}O_{19}$ (M = Cu, Mn, Fe, Ni, Mg) catalysts show the same order of activity as $LaMAl_{11}O_{19}$ (M = Cu, Mn, Fe, Ni, Mg) catalysts. It is indicated that the catalytic activity of these catalysts mainly depends on the M ions.

Fig. 13 shows the results of the H_2-TPR measurements of $Sr_{1-x}La_xMnAl_{11}O_{19}$ (x = 0.2–0.8) catalysts. Obviously, all the catalysts exhibit almost the same H_2-TPR profiles. Except for $Sr_{0.6}La_{0.4}MnAl_{11}O_{19}$ and $Sr_{0.8}La_{0.2}MnAl_{11}O_{19}$ catalysts, these catalysts have a low temperature reduction peak and a high temperature reduction peak, and the reduction peak area of the low temperature reduction peak is much larger than that of the high temperature reduction peak. For $LaMnAl_{11}O_{19}$ catalyst, the low temperature reduction peak is at 435 °C and the high temperature reduction peak is at 927 °C (Fig. 13a). When Sr is added, the low temperature reduction peak shifts to high temperature, and the high temperature reduction peak shifts to low temperature. However, when the Sr content increases, the position of the two reduction peaks remains almost unchanged, and is at about 463 and 897 °C, respectively. Furthermore, the intensity of the two peaks keeps almost unchanged with increasing of Sr content in $Sr_{1-x}La_xMnAl_{11}O_{19}$ hexaaluminates. There are two reduction peaks at 50 and 771 °C, respectively, in $Sr_{0.6}La_{0.4}MnAl_{11}O_{19}$ (Fig. 13d) and a reduction peak at 560 °C in $Sr_{0.8}La_{0.2}MnAl_{11}O_{19}$ (Fig. 13e), indicating that there are other oxygen species in these catalysts.

From Fig. 13, all catalysts begin to be reduced at about 200 °C, namely, the initial reduction temperature of these catalysts remains almost unchanged with various x in $Sr_{1-x}La_xMnAl_{11}O_{19}$ catalysts. At the same time, the reduction peak area of these catalysts also remains almost unchanged with x, suggesting that the catalytic activity of these catalysts is close. From the results of activities as shown in Table 1, it has been found that T_{50} and T_{90} of these catalysts are indeed very close. According to the above results, $Sr_{1-x}La_xMnAl_{11}O_{19}$ (x = 0.2–0.8) catalysts exhibit almost the same redox properties, resulting in close activity of these catalysts.

4. Conclusions

The urea combustion method, as a new preparation method, was applied successfully to prepare hexaaluminate materials, and a series of $AAl_{12}O_{19}$ (A = La, Sr, Ba, Ca, Ce), $AMAl_{11}O_{19}$ (A = La, Sr; M = Cu, Mn, Fe, Ni, Mg) and $Sr_{1-x}La_xMnAl_{11}O_{19}$ (x = 0.2–0.8) hexaaluminates were prepared under the proper preparation conditions. The prepared hexaaluminates had a pure and complete phase structure and relatively high specific surface areas and an excellent catalytic activity for the methane combustion. In $AAl_{12}O_{19}$ (A = La, Sr, Ba, Ca, Ce) hexaaluminates, $CaAl_{12}O_{19}$ had the highest specific surface area of 24.3 $m^2\ g^{-1}$, and $LaAl_{12}O_{19}$ showed the best catalytic activity whose T_{90} was 610 °C. In $LaMAl_{11}O_{19}$ (M = Cu, Mn, Fe, Ni, Mg) hexaaluminates, $LaMgAl_{11}O_{19}$ had the highest specific surface area of 21.6 $m^2\ g^{-1}$, and $LaCuAl_{11}O_{19}$ showed the best catalytic activity whose T_{90} was 533 °C. In $SrMAl_{11}O_{19}$ (M = Cu, Mn, Fe, Ni, Mg) hexaaluminates, $SrMgAl_{11}O_{19}$ had the highest

specific surface area of 18.3 $m^2\ g^{-1}$, and $SrCuAl_{11}O_{19}$ exhibited the best catalytic activity whose T_{90} was 542 °C. In $Sr_{1-x}La_xMnAl_{11}O_{19}$ (x = 0.2–0.8) hexaaluminates, $Sr_{0.2}La_{0.8}MnAl_{11}O_{19}$ showed the best catalytic activity whose T_{90} was 570 °C. The H_2-TPR results showed that there was a corresponding relationship between the catalytic activity in methane combustion and the redox properties of the hexaaluminates. Comparison with the preparation methods reported in literatures, the urea combustion method was an excellent preparation method of the hexaaluminates.

Acknowledgements

Financial funds from the Chinese Natural Science Foundation (Project Nos. 20376005 and 20473009) and the National Basic Research Program of China (Project No. 2005CB221405) are gratefully acknowledged.

Appendix A. Supplementary data

Supplementary data associated with this article can be found, in the online version, at doi:10.1016/j.molcata.2008.05.015.

References

[1] T.V. Choudhary, S. Banerjee, V.R. Choudhary, Appl. Catal. A: Gen. 234 (2002) 1–23.
[2] D.R.A. Betta, Catal. Today 35 (1997) 129–135.
[3] P. Forzatti, G. Groppi, Catal. Today 54 (1999) 165–180.
[4] T.C. Xiao, S.F. Ji, H.T. Wang, K.S. Coleman, M.L.H. Green, J. Mol. Catal. A: Chem. 175 (2001) 111–123.
[5] B. Jang, R.M. Nelson, J.J. Spivey, M. Ocal, R. Oikaci, G. Marcelin, Catal. Today 47 (1999) 103–113.
[6] V.C. Belessi, A.K. Ladavos, P.J. Pomonis, Appl. Catal. B: Environ. 31 (2001) 183–194.
[7] G. Groppi, C. Cristiani, P. Forzatti, Appl. Catal. B: Environ. 35 (2001) 137–148.
[8] S.R. Jansen, H.T. Hintzen, R. Metselaar, J. Solid State Chem. 129 (1997) 66–73.
[9] B.M.J. Smets, J.G. Verlijsdonk, Mater. Res. Bull. 21 (1986) 1305–1310.
[10] H. Inoue, K. Sekizawa, K. Egichi, H. Arai, J. Solid State Chem. 121 (1996) 190–196.
[11] L.C. Yan, L.T. Thompson, Appl. Catal. A: Gen. 171 (1998) 219–228.
[12] Z. Xu, M. Zhen, Y. Bi, K. Zhen, Catal. Lett. 64 (2000) 157–161.
[13] G. Groppi, M. Bellotto, C. Cristiam, P. Forzatti, P.L. Villa, Appl. Catal. A: Gen. 104 (1993) 101–108.
[14] P.O. Thevenin, A.G. Ersson, H.M.J. Kusar, P.G. Menon, S.G. Järås, Appl. Catal. A: Gen. 212 (2001) 189–197.
[15] J.W. Wang, Z.J. Tian, J.G. Xu, Y.P. Xu, Z.S. Xu, L.W. Lin, Catal. Today 83 (2003) 213–222.
[16] A.J. Zarur, J.Y. Ying, Nature 403 (2000) 65–67.
[17] A.J. Zarur, H.H. Hwu, J.Y. Ying, Langmuir 16 (2000) 3042–3049.
[18] S.J. Cho, Y.S. Seo, K.S. Song, J.N. Jeong, S.K. Kang, Appl. Catal. B: Environ. 30 (2001) 351–357.
[19] M.M.A. Sekar, K.C. Patil, J. Mater. Chem. 2 (1992) 739–743.
[20] D.A. Fumo, J.R. Jurado, A.M. Segadães, J.R. Frade, Mater. Res. Bull. 32 (1997) 1459–1470.
[21] P. Bera, S.T. Aruna, K.C. Patil, M.S. Hegde, J. Catal. 186 (1999) 36–44.
[22] E. Flahaut, A. Peigney, C. Laurent, A. Rousset, J. Mater. Chem. 10 (2000) 249–252.
[23] R.D. Purohit, B.P. Sharma, K.T. Pillai, A.K. Tyagi, Mater. Res. Bull. 36 (2001) 2711–2721.
[24] G. Avgouropoulos, T. Ioannides, Appl. Catal. A: Gen. 244 (2003) 155–167.
[25] A. Ringuedé, J.A. Labrincha, J.R. Frade, Solid State Ionics 141–142 (2001) 549–557.
[26] M. Marinsek, K. Zupan, J. Maèek, J. Power Sources 106 (2002) 178–188.
[27] S. Biamino, P. Fino, M. Pavese, C. Badini, Ceram. Int. 32 (2006) 509–513.
[28] G. Avgouropoulos, T. Ioannides, H. Matralis, Appl. Catal. B: Environ. 56 (2005) 87–93.
[29] A. Cordier, A. Peigney, E.D. Grave, E. Flahaut, C. Laurent, J. Eur. Ceram. Soc. 26 (2006) 3099–3111.
[30] T. Tabakova, V. Idakiev, J. Papavasiliou, G. Avgouropoulos, T. Ioannides, Catal. Commun. 8 (2007) 101–106.
[31] A. Civera, M. Pavese, G. Saracco, V. Specchia, Catal. Today 83 (2003) 199–211.
[32] S.E. Dali, J.M. Chockalingam, Mater. Chem. Phys. 70 (2001) 73–77.
[33] R.K. Selvan, C.O. Augustin, L.J. Berchmans, R. Saraswathi, Mater. Res. Bull. 38 (2003) 41–54.
[34] C. Păcurariu, I. Lazău, Z. Ecsedi, R. Lazău, P. Barvinschi, G. Mărginean, J. Eur. Ceram. Soc. 27 (2007) 707–710.
[35] W. Chen, F. Li, J. Yu, L. Liu, Mater. Sci. Eng. B 133 (2006) 151–156.
[36] S.F. Ji, T.C. Xiao, H.T. Wang, E. Flahaut, K.S. Coleman, M.L.H. Green, Catal. Lett. 75 (2001) 65–71.
[37] S. Ji, C. Li, Z. Lei, B. Chen, CN 200310117394 (2003).
[38] S. Ji, C. Li, B. Chen, H. Liu, CN 200410062251 (2004).
[39] J. Kirchnerova, D. Klvana, Catal. Lett. 67 (2000) 175–181.
[40] L. Lietti, C. Cristiani, G. Groppi, P. Forzatti, Catal. Today 59 (2000) 191–204.
[41] P. Artizza, N. Guilhaume, E. Garbowski, Y. Brullé, M. Primet, Catal. Lett. 51 (1998) 69–75.
[42] K. Eguchi, H. Inoue, K. Sekizawa, H. Arai, Stud. Surf. Sci. Catal. 101 (1996) 417–425.
[43] M. Machida, K. Eguchi, H. Arai, J. Catal. 123 (1990) 477–485.
[44] M. Machida, K. Eguchi, H. Arai, J. Catal. 120 (1989) 377–386.
[45] J.G. McCarty, M. Gusman, D.M. Lowe, D.L. Hildenbrand, K.N. Lau, Catal. Today 47 (1999) 5–17.
[46] A. Ersson, K. Persson, I.K. Adu, S.G. Järås, Catal. Today 112 (2006) 157–160.
[47] S. Li, H. Liu, L. Yan, X. Wang, Catal. Commun. 8 (2007) 237–240.
[48] T.F. Yeh, H.G. Lee, K.S. Chu, C.B. Wang, Mater. Sci. Eng. A 384 (2004) 324–330.
[49] W. Chu, W. Yang, L. Lin, Catal. Lett. 74 (2001) 139–144.
[50] P. Artizzu-Duart, J.M. Millet, N. Guilhaume, E. Garbowski, M. Primet, Catal. Today 59 (2000) 163–177.
[51] E.R. Stobbe, B.A. De Boer, J.W. Geus, Catal. Today 47 (1999) 161–167.
[52] Z. Xu, M. Zhen, Y. Bi, K. Zhen, Appl. Catal. A: Gen. 198 (2000) 267–273.